



Contents lists available at ScienceDirect

Journal of Non-Crystalline Solids

journal homepage: www.elsevier.com/locate/jnoncrysol

Crystallization process on amorphous GeTeSb samples near to eutectic point Ge₁₅Te₈₅

J. Rocca, M. Erazú, M. Fontana *, B. Arcondo

Laboratorio de Sólidos Amorfos, INTECIN, Facultad de Ingeniería, Universidad de Buenos Aires – CONICET, Paseo Colon 850, 1063 Buenos Aires, Argentina

ARTICLE INFO

Article history:
Available online 20 July 2009

PACS:
61.05.cp
64.70.dg
61.43.Dq

Keywords:
Crystallization
X-ray diffraction
Calorimetry

ABSTRACT

One of most important properties of some tellurium-based chalcogenide glasses is the optical and electrical switching between two states: the glass and the crystalline state. The understanding in these systems of the glass to crystal transition and its transformation kinetics is essential for their application in non-volatile memories. GeTeSb and GeTe amorphous samples of compositions close to the eutectic point Ge₁₅Te₈₅ were obtained by rapid solidification from the liquid state employing melt spinning technique. The glass forming ability of this system, for this cooling technique, is restricted to a small composition range nearby the binary eutectic. The crystallization kinetics of the samples was studied by means of differential scanning calorimetry (DSC) under both isothermal and continuous heating regimes. The quenched samples and the crystallization products have been characterized by X-ray diffraction with Cu(K α) radiation. The crystallization temperature, activation energy, crystallization enthalpy and the dependence of these properties on concentration are reported. The crystallization study of Ge₁₅Te₈₅ glasses shows: a primary crystallization of Te superimposed with a secondary crystallization of GeTe. The addition of Sb (5 at.%) to the eutectic point Ge₁₅Te₈₅ modifies this behavior: the crystallization of Ge₁₃Sb₅Te₈₂ glasses consists on the crystallization of Te and Ge₂Sb₂Te₅. The crystallization of the ternary glasses was modeled.

© 2009 Elsevier B.V. All rights reserved.

1. Introduction

GeSbTe amorphous films are widely used in rewritable compact disks (CD-RW), digital versatile disks (DVD-RW) and are found to be suitable for electrical memories (i.e.: non-volatile memories) [1]. In optical applications, information is recorded using the fact that a thin film of this system can be reversibly switched by laser heating between the amorphous and the crystalline state [2,3]. The amorphous films with compositions on the GeTe–Sb₂Te₃ pseudo–binary system are utilized in these massive memory storage applications. The compounds Ge₂Sb₂Te₅, GeSb₂Te₄ and GeSb₂Te₇ of this pseudo–binary system have been extensively studied and have the following characteristics: high thermal stability at room temperature, high crystallization rate and very good reversibility between amorphous and crystalline phases. Yamada et al. [4] reported that Ge₂Sb₂Te₅, GeSb₂Te₄ and GeSb₂Te₇ compounds present two crystalline states, one is a meta-stable face centered cubic and the other is a stable hexagonal structure. Ge₂Sb₂Te₅ composition (fcc cell – amorphous material transition) exhibits the best performance when used in DVD-RAM in terms of stability and speed [5–8]. However, glasses GeTe–Sb₂Te₃ pseudo–binary system cannot be

obtained by rapid solidification from the liquid state; a higher cooling rate is needed.

The glass forming ability of GeTeSb system, for rapid solidification from the liquid, is restricted to a small composition range near the binary eutectic Ge₁₅Te₈₅[9]. GeTe system has a eutectic point at $T_e \sim 648$ K formed by the co-precipitation of GeTe and Te. The crystallization kinetic of these ternary composition samples has not been studied yet, as far as we know.

The aim of this work is to analyze the influence of the addition of Sb on the thermal stability of glasses which compositions lie close to the binary eutectic Ge₁₅Te₈₅, as well as the crystallization kinetics and crystallization products of these glasses. To answer these questions, a ternary composition was chosen: Ge₁₃Sb₅Te₈₂. The main mechanisms that drive the crystallization process of this ternary glass are analyzed and compared with those acting on the binary eutectic.

2. Experimental

Samples with compositions Ge₁₅Te₈₅ and Ge₁₃Sb₅Te₈₂ were synthesised from the elemental blend of Ge, Sb and Te (4 N purity) in stoichiometric proportions located in quartz ampoules previously evacuated. Fusion and homogenization of the alloys was performed in a furnace at 700 °C for 8 h. The process to produce

* Corresponding author. Tel.: +54 11 4343 0891; fax: +54 11 4331 1852.
E-mail address: mfontan@fi.uba.ar (M. Fontana).

amorphous samples was done in two steps. Firstly, melts were quenched by immersing into an ice–water bath (melt quenching technique - **MQ**). Secondly, the obtained ingots were melted again and then were rapidly quenched employing melt spinning technique (**MS**). Small and fragile flakes were obtained.

Thermal properties were measured using a power compensation differential scanning calorimeter (**DSC**) under dynamic Ar atmosphere. **DSC** experiments were carried out employing always the same mass (5.00 ± 0.05 mg) to avoid the effects of temperature gradients between the furnace and the sample, and within the sample itself. The samples were sealed in aluminum pans. Continuous heating experiments were performed from 323 K to about 623 K at scan rates $\beta = 5, 10, 20, 40$ and 80 K/min. Isothermal experiments of $\text{Ge}_{13}\text{Sb}_5\text{Te}_{82}$ samples were carried out at several temperatures (443, 448 and 453 K). In these measurements, previous heating of the amorphous samples from room temperature to the annealing temperature was performed at a rate of 80 K/min.

The quenched samples and their crystallization steps were analyzed by X-ray diffraction at room temperature in a Θ – Θ diffractometer using monochromatized $\text{Cu}(K\alpha)$ radiation. Partially-crystallized $\text{Ge}_{13}\text{Sb}_5\text{Te}_{82}$ samples (with 10% of crystalline fraction) were examined using optical microscopy.

3. Results

X-ray diffractograms (**XRD**) of the $\text{Ge}_{15}\text{Te}_{85}$ and $\text{Ge}_{13}\text{Sb}_5\text{Te}_{82}$ samples, rapidly quenched by both techniques **MQ** and **MS**, are shown in Figs. 1 and 2. The cooling rate of the **MQ** technique is not enough to produce amorphous samples, whereas the **XRD** obtained for the samples cooled by the **MS** technique have broad peaks due to an amorphous phase. Figs. 1 and 2 also show **XRD** obtained after thermal annealing of samples $\text{Ge}_{15}\text{Te}_{85}$ and $\text{Ge}_{13}\text{Sb}_5\text{Te}_{82}$.

Fig. 3 shows the differential scanning calorimetry (**DSC**) curves (dH/dT vs T , where H is the enthalpy and T the temperature), for a heating rate of 20 K/min, of samples $\text{Ge}_{15}\text{Te}_{85}$ and $\text{Ge}_{13}\text{Sb}_5\text{Te}_{82}$, rapidly quenched by the **MS** technique. **XRD** of $\text{Ge}_{15}\text{Te}_{85}$ and $\text{Ge}_{13}\text{Sb}_5\text{Te}_{82}$ samples were obtained at different steps of the crystallization process (see Fig. 3): (i) after annealing at a heating

rate of 20 K/min up to point A (in Fig. 3) for the binary sample and point B (in Fig. 3) for the ternary sample (samples were then cooled down to room temperature at a rate of 200 K/min) and (ii) after the crystallization processes ended. **XRD** were also obtained after isothermal annealings.

A glass transition is detected in both samples. The glass temperature T_g and the heat capacity change ΔC_p in the glass transition were obtained and the results are shown in Table 1.

Two main exothermic peaks can be observed in $\text{Ge}_{15}\text{Te}_{85}$ **DSC** curve. They correspond to a primary crystallization of the Te phase and a secondary crystallization (with overlapping process) of the GeTe phase as it is shown in the **XRD** of Fig. 1 (see DSC1 and DSC2).

DSC curve of the $\text{Ge}_{13}\text{Sb}_5\text{Te}_{82}$ sample shows a single exothermic peak corresponding to the crystallization of Te phase (with many diffraction lines) and other non identified phase; a few remaining diffraction peaks are associated to the stable ternary phase $\text{Ge}_2\text{Sb}_2\text{Te}_5$ with a hexagonal cell [8] (see DSC3 in the Fig. 2). The crystallization of these phases is not simultaneous, only Te crystalline phase is detected by X-ray diffraction in the first steps (about 10% of crystalline fraction, point B in Fig. 3) of this single crystallization peak (see DSC1 in Fig. 2). Optical micrograph of the $\text{Ge}_{13}\text{Sb}_5\text{Te}_{82}$ sample after the thermal treatments up to point B (in Fig. 3) is shown in Fig. 4. The structure observed consists of spheroidal Te crystal particles (dark) in a matrix of glass (grey).

Te phase and an only incipient diffraction line corresponding to $\text{Ge}_2\text{Sb}_2\text{Te}_5$ (hexagonal cell) are detected by X-ray in the ternary sample under isothermal regime (see DSC2 in Fig. 2). The dependence with the heating rate of the crystallization onset temperature T_x , the peak temperature, T_p , (I and II), and the enthalpy of the crystallization (ΔH_c) are also shown in Table 1. Since on increasing β , the transformations shift to higher temperatures, evidencing the well-known characteristic of activated processes [10]. The apparent activation energy, E_a , for the crystallization processes was deduced by the Kissinger method [11] (from continuous heating data) and the results are shown in Table 1.

Kauzmann ratio T_g/T_m [12] is the most extensively used parameter for determining the glass forming ability (**GFA**). T_g/T_m is about 2/3 for good glass formers. Considering that the melting temperature T_m is close to the GeTe eutectic temperature ($T_m = 648$ K) we

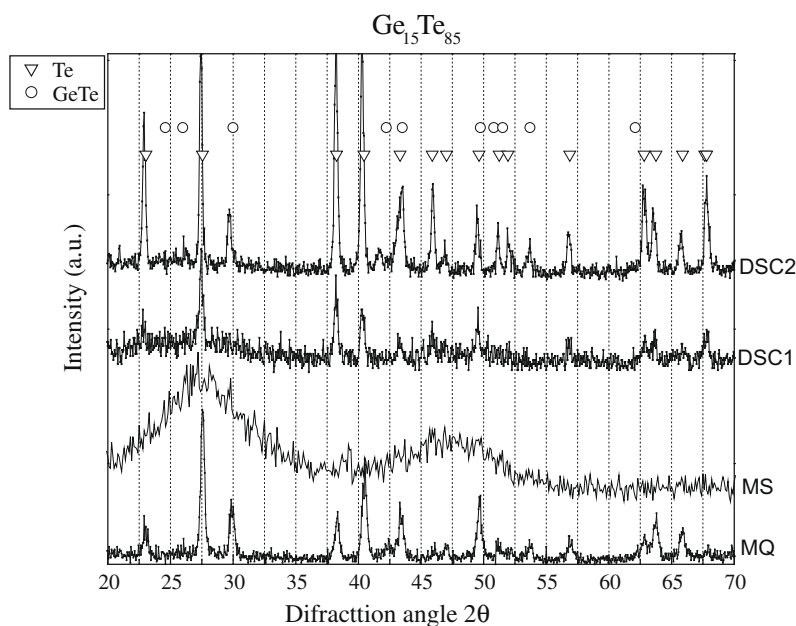


Fig. 1. **XRD** of the $\text{Ge}_{15}\text{Te}_{85}$ sample rapidly quenched and carried out after thermal treatments. The peaks corresponding to the crystalline phase are indicated. The symbols indicate the X-ray patterns of the crystalline phases: Te and GeTe. **MQ**: rapidly quenched by melt quenching technique, **MS**: rapidly quenched by melt spinning technique, **DSC1**: after the thermal treatments up to point A in Fig. 3 (at 20 K/min), **DSC2**: after continuous heating DSC experiment for the whole T range.

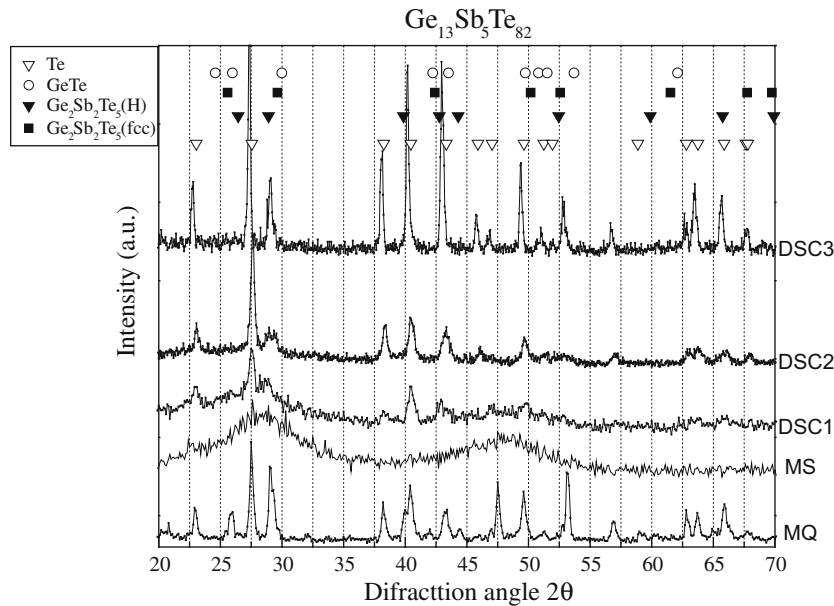


Fig. 2. XRD of the $\text{Ge}_{13}\text{Sb}_5\text{Te}_{82}$ sample rapidly quenched and carried out after thermal treatments. The peaks corresponding to the crystalline phase are indicated. The symbols indicate the X-ray patterns of the crystalline phases: Te, GeTe, $\text{Ge}_2\text{Sb}_2\text{Te}_5$ (Hexagonal structure) and $\text{Ge}_2\text{Sb}_2\text{Te}_5$ (fcc structure). **MQ**: rapidly quenched by melt quenching technique, **MS**: rapidly quenched by melt spinning technique, **DSC1**: after the thermal treatments up to point **B** in Fig. 3 (at 20 K/m), **DSC2**: after isothermal DSC experiment, **DSC3**: after continuous heating DSC experiment for the whole T range.

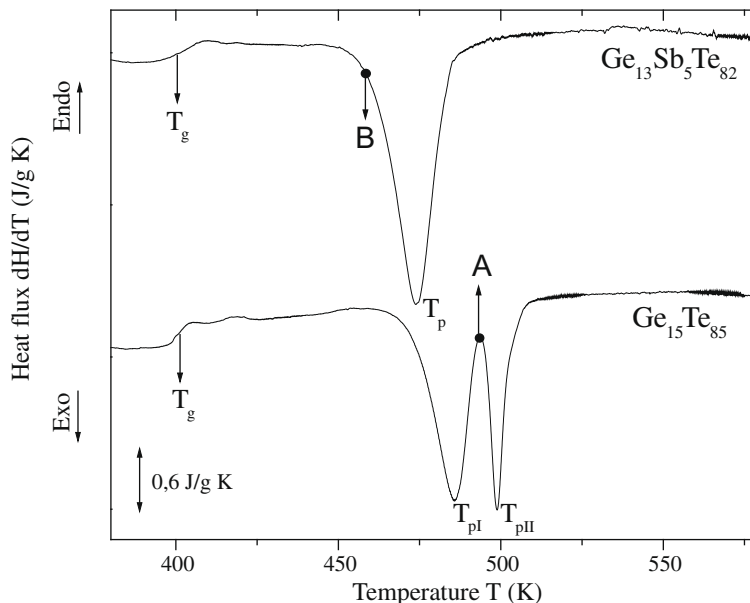


Fig. 3. DSC curves (dH/dT vs T) of the $\text{Ge}_{15}\text{Te}_{85}$ and $\text{Ge}_{13}\text{Sb}_5\text{Te}_{82}$ samples at a heating rate of 20 K/min. The **A** and **B** points (in $\text{Ge}_{15}\text{Te}_{85}$ and $\text{Ge}_{13}\text{Sb}_5\text{Te}_{82}$ samples respectively) indicate the reached temperature before the XRD experiment (at room temperature).

can determine T_g/T_m , which is in the range between 0.61 and 0.64. Therefore we can conclude that the samples studied are good glass forming alloys. Recently, a new criterion for evaluating **GFA** was proposed [13]. These authors show that the **GFA** is strongly correlated with the parameter $\gamma = T_x/(T_g + T_m)$. γ is in the range 0.35–0.50 for most bulk metallic glasses. For the studied alloys γ results in the range 0.41–0.44 indicating also a good **GFA**. The glass stability can be analyzed with a parameter of Hruby $K_{gl} = (T_x - T_g)/(T_m - T_x)$ [14–15]. Alloys with larger K_{gl} show a higher stability against crystallization on heating indicating a better **GFA** (for $K_{gl} \sim 0.1$, the preparation of glasses is very difficult whereas for $K_{gl} \sim 0.5$ glasses are obtained by quenching in air [16]). The values

of K_{gl} for the different heating rates are in the range 0.24–0.31 for the $\text{Ge}_{15}\text{Te}_{85}$ glass and in the range 0.24–0.26 for the $\text{Ge}_{13}\text{Sb}_5\text{Te}_{82}$ sample. This result shows that the binary amorphous alloy is a little more stable than the ternary glass.

4. Discussion

Comparing the crystallization results obtained for the binary eutectic amorphous sample with previous works [17–18], we observe: (a) the reported crystalline phases (Te and GeTe) are the same, (b) the appearance of the DSC curve is similar, (c) the glass and crystallization temperatures are different from the reported

Table 1

Heating rate dependence of the calorimetric parameters: the glass temperature T_g , the heat capacity change ΔC_p in the glass transition, the crystallization onset temperature T_x , the peak crystallization temperature T_p , the crystallization enthalpy ΔH_c , and the activation energy E_a of the samples $\text{Ge}_{15}\text{Te}_{85}$ and $\text{Ge}_{13}\text{Te}_{82}\text{Sb}_5$. In the case of the binary sample, ΔH_c is the sum of the crystallization enthalpy of the peaks I and II.

Sample	Glass transition			Crystallization peak				Activation energy E_a (kJ/mol)	
	β (K/m)	T_g (K)	ΔC_p (J/gK)	T_x (K)	T_{pl} (K)	T_{pII} (K)	ΔH_c (J/g)	I peak	II peak
$\text{Ge}_{15}\text{Te}_{85}$	5	–	–	446	473	488	43		
	10	405	0.32	452	478	493	45		
	20	408	0.29	459	486	499	36	190	262
	40	412	0.32	464	491	503	40		
	80	416	0.23	471	499	509	42		
$\text{Ge}_{13}\text{Te}_{82}\text{Sb}_5$	5	399	0.22	434	463		30		
	10	401	0.30	449	470		36		
	20	403	0.27	450	474		36	207	
	40	406	0.22	452	480		38		
	80	408	0.23	458	487		44		

$\Delta(T_g) = 3$ K, $\Delta(\Delta C_p) = 0.02$ J/gK, $\Delta(T_x) = 2$ K, $\Delta(T_p) = 0.5$ K, $\Delta(\Delta H_c) = 5\%$ and $\Delta(E_a) = 5\%$.



Fig. 4. Optical micrograph of the $\text{Ge}_{13}\text{Sb}_5\text{Te}_{82}$ sample after the thermal treatments up to point **B** in Fig. 3 (Optical magnification: 1000 \times).

values in less than 10 K (d) the activation energy E_a of the first crystallization peak is similar whereas E_a associated to the crystallization of GeTe phase (shown in Table 1) is considerably different from the reported values ($E_a = 345 \pm 26$ kJ/mol [17]).

Consequences of adding Sb (5 at.%) to the binary eutectic are:

- first of all, the crystallization temperature in $\text{Ge}_{13}\text{Sb}_5\text{Te}_{82}$ sample is lower (about 10 K) than those of binary composition,
- although Te crystal is the main crystallization product in both samples, the secondary crystallization is different (GeTe phase in the binary composition, $\text{Ge}_2\text{Sb}_2\text{Te}_5$ (hexagonal cell) in the ternary alloy). Moreover, the appearance of the stable phase $\text{Ge}_2\text{Sb}_2\text{Te}_5$ at this temperature (about 450–485 K) is in agreement with experiments of Yamada et al. [4]. They observed that the transition between metastable phase (fcc cell) and stable phase (hexagonal cell) occurs at 473 K.
- the appearance of the DSC curve is different (two overlapped exothermic peaks in the binary composition, one exothermic peak in the $\text{Ge}_{13}\text{Sb}_5\text{Te}_{82}$ sample),
- E_a associated to the $\text{Ge}_{13}\text{Sb}_5\text{Te}_{82}$ sample crystallization is similar to E_a of the Te crystalline phase in the eutectic composition (primary crystallization). Furthermore, this value ($E_a = 207$ kJ/mol) is proper because it is intermediate between E_a of the crystallized phases (E_a for Te crystalline

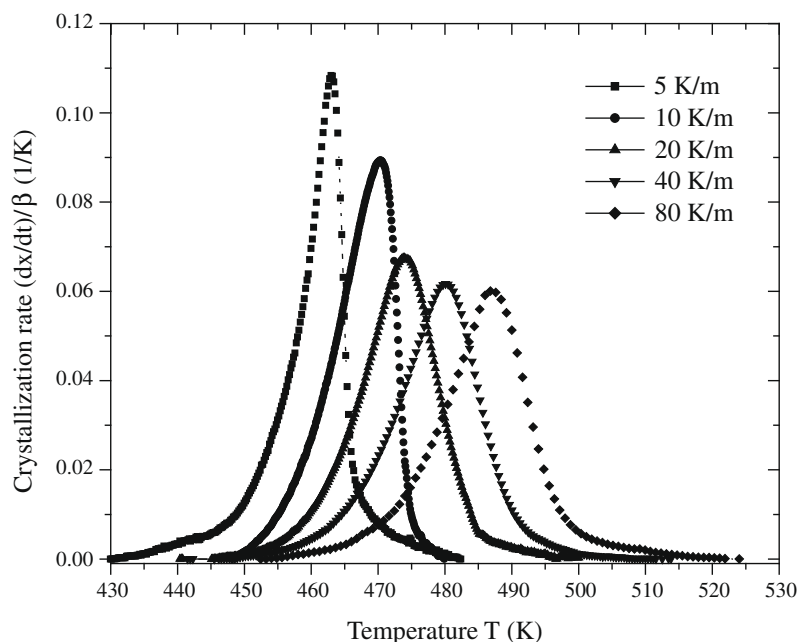


Fig. 5. Crystallization rate dx/dt (normalized by the heating rate β) vs. Temperature obtained for the crystallization of the $\text{Ge}_{13}\text{Sb}_5\text{Te}_{82}$ amorphous sample at different heating rates.

phase in binary eutectic, that is $E_a = 190$ kJ/mol, and $E_a = 215$ kJ/mol obtained for the crystallization of $\text{Ge}_2\text{Sb}_2\text{Te}_5$ thin film [4,6],

(e) the glass temperature is similar in both compositions.

The temperature dependence of the crystallization rate dx/dt for $\text{Ge}_{13}\text{Sb}_5\text{Te}_{82}$ sample is shown in Fig. 5. A clear dependence of dx/dt curve appearance on the heating rate β can be observed. This fact let us conclude that the $\text{Ge}_{13}\text{Sb}_5\text{Te}_{82}$ sample crystallization is not isokinetic (a process is isokinetic if it does not depend on the kinetic parameters [19]). Moreover, following above ideas, the ternary sample crystallization is constituted by leastwise two processes being the Te crystallization the most important and the earliest process.

4.1. Initial steps of crystallization

Following previous work, [20–22,27] the initial steps of the formation of crystals (crystalline fraction $x < 0.1$) are modeled from experimental calorimetric data. As mentioned above, the crystallization of these glasses is complex. However, the first steps of the crystallization of the samples can be modeled assuming homogeneous nucleation with frequency, I , followed by three-dimensional interface-controlled crystal growth of the crystal with a rate, u [24].

The classical equations used are expressed as [22,25,26]:

$$I(T) = [4(\sigma/RT)^{1/2}N_v \cdot b/\eta] \cdot \exp(-\Delta G^*/RT), \quad (1)$$

$$u(T) = (a_o \cdot \lambda \cdot b/\eta) \cdot [1 - \exp(-\Delta G/RT)], \quad (2)$$

$$b = kT/(3\pi L^2 a_o^3),$$

where N_v is the mean density of atoms, a_o the mean atomic diameter, T the temperature, σ the molar interface energy between the nucleus and the liquid, λ is the product of the fraction of surface sites where atoms are preferentially added and the length of the interface in units of a_o , L is the mean interfacial thickness in units of a_o , and η is the viscosity which dependence on T obeys a Vogel–Fulcher expression [20,21]:

$$\eta = \eta_o \exp(A/(T - T_o)), \quad (3)$$

ΔG^* is the Gibbs free-energy of formation of a nucleus of critical size [14,15]:

$$\Delta G^* = 16\pi\sigma^3/(3\Delta G^2), \quad (4)$$

where ΔG is the Gibbs free-energy difference between the supercooled liquid and the crystal [26,27]:

$$\Delta G = \Delta H_m \cdot [(1 - T_r) \cdot (1 - \Gamma) - \Gamma T_r \ln(T_r)], \quad (5)$$

Here $T_r = T/T_m$, $\Gamma = \Delta C_p/\Delta S_m$, ΔC_p is the heat capacity difference between the liquid and the crystal, T_m , ΔS_m and ΔH_m are the melting temperature, melting entropy and melting enthalpy.

For a process of homogeneous nucleation with frequency, I , followed by three-dimensional interface-controlled crystal growth of the crystal with a rate, u , the time temperature transformation (TTT) and temperature-heating rate-transformation (THRT) diagrams can be calculated using [20–23]:

$$x(T, t) = 1 - \exp(-(\pi/3) \cdot I(T) \cdot u(T)^3 \cdot t^4) \quad (6)$$

[TTT diagrams – nucleation and growth],

with t the time,

$$x(T, \beta) = 1 - \exp(-\beta^{-1} \cdot \int_0^T I(T') \cdot v_{ng}(T', T) \cdot dT') \quad (7)$$

× [THRT diagrams – nucleation and growth],

with β the heating rate and $v_{ng}(T', T)$ the volume at temperature T of a nucleus formed at temperature T' , given by:

$$v_{ng}(T', T) = (4\pi/3)[\beta^{-1} \cdot \int_{T'}^T u(T') \cdot dT']^3, \quad (8)$$

4.2. Initial steps of the $\text{Ge}_{15}\text{Te}_{85}$ and $\text{Ge}_{13}\text{Sb}_5\text{Te}_{82}$ sample crystallization

As mentioned above, we assume that only Te phase crystallizes in the initial steps of the $\text{Ge}_{13}\text{Sb}_5\text{Te}_{82}$ sample crystallization.

Table 2

Estimated and assessed values used to model the first crystallization steps of the samples $\text{Ge}_{15}\text{Te}_{85}$ and $\text{Ge}_{13}\text{Sb}_5\text{Te}_{82}$.

Estimated parameters:		
ΔH_m (kJ/mol)	17.0	
T_m (K)	648	
Γ	1.2	
σ	0.33 ΔH_m	
a_o (m)	$2.8 \cdot 10^{-10}$ m	
L^2/λ	10	
Fitted parameters:		
Sample	$\text{Ge}_{15}\text{Te}_{85}$	$\text{Ge}_{13}\text{Sb}_5\text{Te}_{82}$
N_v/L^2 ($1/\text{m}^3$)	1.27×10^{17}	1.16×10^{19}
± 10%		
$\eta(T_m)(\text{P})$	0.010	
A (K)	1250.0	
± 5%		
T_o (K)	370	
± 4		

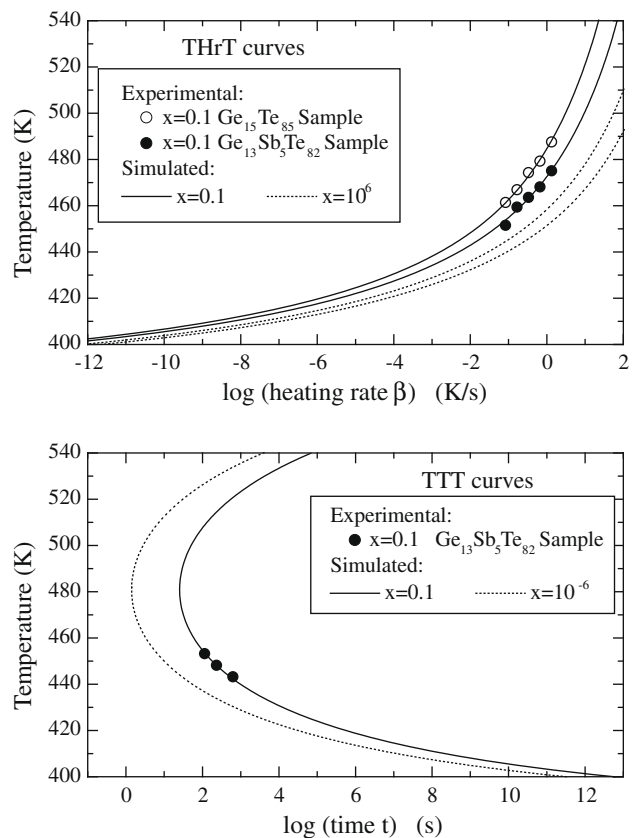


Fig. 6. Calculated temperature-heating rate-transformation (THRT) and temperature-time-transformation (TTT) curves for different values of the crystallized fraction ($x = 10^{-6}$, and 0.1) as well as the experimental data obtained for $x = 0.1$ for the crystallization of the $\text{Ge}_{13}\text{Sb}_5\text{Te}_{82}$ sample and the first crystallization peak of the $\text{Ge}_{15}\text{Te}_{85}$ sample (associated to the crystallization of the Te phase).

The first steps of the crystallization of the samples $\text{Ge}_{15}\text{Te}_{85}$ and $\text{Ge}_{13}\text{Sb}_5\text{Te}_{82}$ were modeled assuming homogenous nucleation followed by three-dimensional interface-controlled crystal growth. We calculated the TTT and THRT curves using calorimetric data obtained **under both isothermal and continuous heating rate regimes** in the case of the ternary sample, whereas only **continuous heating data** were used in the $\text{Ge}_{15}\text{Te}_{85}$ sample. We assumed that some parameters (ΔH_m , σ , a_0 , $L^2\lambda$, T_m and Γ) used in Eqs. (1)–(8) are the same in both samples and some of those (ΔH_m , σ , Γ , a_0 , $L^2\lambda$) are obtained from previous works for the crystallization of Te phase in $\text{Ga}_{20}\text{Te}_{80}$ and GaSnTe alloys [27–28]. Some parameters (T_m and Γ) in Eqs. (1)–(8) were determined or estimated as follow: T_m is assumed the same in both samples and equal to melting temperature of the binary eutectic, Γ was estimated using ΔC_p , ΔH_m and T_m . We assumed that the viscosity parameters ($\eta(T_m)$, A and T_o) are the same in both samples because the glass temperature and the melting temperature are similar and the samples composition is close. The different compositions only modify the parameter N_v/L^2 .

The parameters (N_v/L^2 , $\eta(T_m)$, A and T_o) were fitted using Eqs. (6) and (7) to reproduce the experimental DSC data ($x = 0.1$) in both samples with an additional condition: $\eta(T_g) \sim 10^{13}$ P.

Estimated as well as fitted parameters are given in Table 2. Calculated temperature-heating rate (THRT) and time temperature transformation (TTT) curves for different crystallized fractions ($x = 10^{-6}$ and 0.1) as well as experimental data obtained for $x = 0.1$ are reported in Fig. 6. The agreement between the calculated curve and the experimental data is very good.

5. Conclusions

The glass forming ability of GeTeSb system, for rapid solidification from the liquid, is restricted to a small composition range near the binary eutectic $\text{Ge}_{15}\text{Te}_{85}$. The crystallization of $\text{Ge}_{13}\text{Sb}_5\text{Te}_{82}$ amorphous samples is mainly governed by the crystallization of Te phase, so is the binary eutectic composition. The addition of Sb (5 at.%) to the eutectic binary generates that the ternary amorphous alloy is less stable than the binary eutectic (lower crystallization temperature) and modifies the secondary crystallization observing the appearance of the stable hexagonal phase $\text{Ge}_2\text{Sb}_2\text{Te}_5$. $\text{Ge}_{13}\text{Sb}_5\text{Te}_{82}$ sample crystallization is not isokinetic. The first steps of the Te phase crystallization are modeled considering that the

changes in composition only modify the nucleation frequency pre-exponential factor (parameter N_v/L^2). The model proposed fits the experimental data as a process of homogeneous nucleation and 3-D growth controlled by the interface.

References

- [1] Z. Sun, J. Zhou, R. Ahuja, Phys. Rev. Lett. 96 (2006) 55507/1–55507/4.
- [2] N. Yamada, T. Matsunaga, J. Appl. Phys. 88 (12) (2000) 7020.
- [3] J.A. Kalb, F. Spaepen, M. Wuttig, J. Appl. Phys. 98 (2005) 54910/1–54910/10.
- [4] N. Yamada, E. Ohno, K. Nishiuchi, N. Akahira, M. Takao, J. Appl. Phys. 69 (5) (1991) 2849.
- [5] M. Lankhorst, B. Ketelaars, R. Wolters, Nat. Mater. 4 (2005) 347.
- [6] M. Wuttig, D. Lusebrink, D. Wamwangi, W. Welnic, M. Gilleben, R. Dronskowski, Nat. Mater. 6 (2007) 122.
- [7] G. Park, J. Kwon, W. Jo, T. Kim, J. Zuo, Y. Khang, J. Appl. Phys. 102 (2007) 13524/1–13524/5.
- [8] T. Matsunaga, N. Yamada, Y. Kubota, Acta Crystall. B – Stru. 60 (2004) 685.
- [9] P. Lebaudy, J.M. Saiter, J. Grenet, M. Belhadi, C. Vautier, Mat. Sci. Eng. A 132 (1991) 273.
- [10] J.W. Christian, Theory of Transformations in Metals and Alloys, Pergamon, Oxford, 1975.
- [11] H.E. Kissinger, Anal. Chem. 29 (1957) 1702.
- [12] W. Kauzmann, Chem. Rev. 43 (1948) 219.
- [13] Z.P. Lu, C.T. Liu, Acta Mater. 50 (2002) 3501.
- [14] A. Hruby, Czech. J. Phys. B 22 (1972) 1187.
- [15] K. Biswas, S. Venkataraman, W. Zhang, S. Ram, J. Eckert, J. Appl. Phys. 100 (2006) 023501.
- [16] C.A. Majid, Internal Report IC/82/131, International Centre for Theoretical Physics, Trieste, Italy, 1982.
- [17] I. Kaban, E. Dost, W. Hoyer, J. Alloys Compd. 379 (2004) 166.
- [18] W. Hoyer, I. Kaban, P. Jovari, E. Dost, J. Non-Cryst. Solids 338–340 (2004) 565.
- [19] M. Fontana, B. Arcondo, M.T. Clavaguera-Mora, N. Clavaguera, J. Non-Cryst. Solids 353 (2007) 2131.
- [20] M.T. Clavaguera-Mora, J. Alloys Compd. 220 (1995) 197.
- [21] J.A. Diego, M.T. Clavaguera-Mora, N. Clavaguera, Mater. Sci. Eng. A 179&180 (1994) 526.
- [22] M.T. Clavaguera-Mora, N. Clavaguera, D. Crespo, T. Pradell, Prog. Mater. Sci. 47 (2002) 559.
- [23] A. Ureña, M. Fontana, B. Arcondo, M.T. Clavaguera-Mora, N. Clavaguera, J. Non-Cryst. Solids 304 (2002) 306.
- [24] M. Fontana, B. Arcondo, M.T. Clavaguera-Mora, N. Clavaguera, Philos. Mag. B 80 (2000) 1833.
- [25] D. Turnbull, J. Appl. Phys. 21 (1950) 1022.
- [26] J.H. Perepezco, in: R. Mehrabian, B.H. Kear, M. Cohen (Eds.), Rapid Solidification Processing Principles and Technologies, Claitor's, Baton Rouge, LA, 1980, P. 56.
- [27] M. Fontana, B. Arcondo, M.T. Clavaguera-Mora, N. Clavaguera, J.M. Grenèche, J. Appl. Phys. 88 (6) (2000) 3276.
- [28] N. Clavaguera, M.T. Clavaguera-Mora, M. Fontana, J. Mater. Res. 13 (1998) 744.